

## CHARACTERIZATION OF (CuO-Fe<sub>2</sub>O<sub>3</sub>) CERAMICS WITH THREE DIFFERENT COMPOSITIONS SINTERED AT 1100 °C FOR NTC THERMISTOR

Dani Gustaman Syarif<sup>1</sup> and Engkir Sukirman<sup>2</sup>

<sup>1</sup>Nuclear Technology Center for Materials and Radiometry (PTRKN) - BATAN  
Jl. Tamansari 71, Bandung 40132

<sup>2</sup>Technology Center for Nuclear Industry Materials (PTBIN) - BATAN  
Kawasan Puspiptek, Serpong 15314, Tangerang

### ABSTRACT

**CHARACTERIZATION OF (CuO-Fe<sub>2</sub>O<sub>3</sub>) CERAMICS WITH THREE DIFFERENT COMPOSITIONS SINTERED AT 1100 °C FOR NTC THERMISTOR.** The formation of (CuO-Fe<sub>2</sub>O<sub>3</sub>) ceramics for NTC thermistors based on CuO-Fe<sub>2</sub>O<sub>3</sub> phase diagram has been studied. The ceramics were produced by pressing an homogeneous mixture of powder of (50 mole % CuO and 50 mole % Fe<sub>2</sub>O<sub>3</sub> as composition 1), (40 mole % CuO and 60 mole % Fe<sub>2</sub>O<sub>3</sub> as composition 2) and (34 mole % CuO and 66 mole % Fe<sub>2</sub>O<sub>3</sub> as composition 3) and sintering the pressed powder at 1100 °C for 2 hours in air with cooling rate of 10 °C/minutes. Electrical characterization was performed by measuring electrical resistivity of the ceramics at various temperatures (25 °C - 100 °C). Analyses of microstructure and crystal structure were carried out by using optical microscope and x-ray diffractometer (XRD), respectively. The x-ray diffraction (XRD) analyses showed that the ceramics of composition 1 and 3 were composed of tetragonal spinel and that of composition 2 was composed of cubic spinel. Hematite second phase was found in the ceramic of composition 3. According to the optical microscopy data, it was known that the ceramics having three different microstructures have been produced. Very large rounded grains were observed in the ceramic of composition 1, polygonal grains were observed in that of composition 2 and very small grains were seen in that of composition 3. According to the electrical data, it was known that the ceramics having thermistor constant (B) between 2000 K and 5000 K have been produced. It was known also that the room temperature resistivity ( $\rho_{RT}$ ) and thermistor constant (B) increased with the increase of Fe<sub>2</sub>O<sub>3</sub> content. The value of B and  $\rho_{RT}$  of the produced (CuO-Fe<sub>2</sub>O<sub>3</sub>) ceramics fits the market requirement.

**Key words :** Thermistor, NTC, CuO-Fe<sub>2</sub>O<sub>3</sub>, phase diagram

### ABSTRAK

**KARAKTERISASI KERAMIK (CuO-Fe<sub>2</sub>O<sub>3</sub>) DENGAN TIGA KOMPOSISI BERBEDA YANG DISINTER PADA SUHU 1100 °C UNTUK TERMISTOR NTC.** Pembentukan keramik (CuO-Fe<sub>2</sub>O<sub>3</sub>) untuk termistor NTC berdasarkan diagram fasa CuO-Fe<sub>2</sub>O<sub>3</sub> telah dipelajari. Keramik dibuat dengan mengepres campuran homogen dari (50 % mol CuO dan 50 % mol Fe<sub>2</sub>O<sub>3</sub> sebagai komposisi 1), (40 % mol CuO dan 60 % mol Fe<sub>2</sub>O<sub>3</sub> sebagai komposisi 2) dan (34 % mol CuO dan 66 % mol Fe<sub>2</sub>O<sub>3</sub> sebagai komposisi 3), lalu menyinter serbuk yang telah dipres pada suhu 1100 °C selama 2 jam di udara dengan kecepatan pendinginan sebesar 10 °C/menit. Karakterisasi listrik dilakukan dengan cara mengukur resistifitas listrik keramik pada berbagai suhu (25 °C sampai dengan 100 °C). Analisis strukturmikro dan strukturmikro kristal masing-masing dilakukan menggunakan mikroskop optik dan difraktometer sinar-X (XRD). Analisis difraksi sinar-X (XRD) memperlihatkan bahwa keramik dari komposisi 1 dan komposisi 3 berstruktur kristal *spinel* tetragonal dan keramik dari komposisi 2 berstruktur kristal *spinel* kubik. Fasa kedua hematit ditemukan pada keramik dari komposisi 3. Sesuai data mikroskop optik, diketahui bahwa keramik dengan tiga jenis strukturmikro telah dapat dibuat. Butir yang cenderung bulat yang sangat besar ditemukan pada keramik dari komposisi 1, butir poligon ditemukan pada keramik dari komposisi 2 dan butir yang sangat kecil terlihat pada keramik dari komposisi 3. Sesuai data listrik, diketahui bahwa keramik yang memiliki konstanta termistor (B) antara 2000 K dan 5000 K telah dapat dibuat. Juga diketahui bahwa resistifitas listrik suhu ruang ( $\rho_{RT}$ ) dan konstanta termistor (B) bertambah dengan penambahan kandungan Fe<sub>2</sub>O<sub>3</sub>. Harga B dan  $\rho_{RT}$  dari keramik (CuO-Fe<sub>2</sub>O<sub>3</sub>) yang telah dibuat, memenuhi kebutuhan pasar.

**Kata kunci :** Termistor, NTC, CuO-Fe<sub>2</sub>O<sub>3</sub>, diagram fasa

## INTRODUCTION

NTC thermistors are widely used in the world due to their potential use for many applications such as temperature measurement, circuit compensation, suppression of inrush-current, flow rate sensor and pressure sensor in many sectors [1]. It is well known that most NTC thermistors are produced from spinel ceramics based on transition metal oxides with general formula of AB<sub>2</sub>O<sub>4</sub> where A is metal ion in tetrahedral position and B is metal ions in octahedral position [3-10]. Many studies have been done to get new NTC thermistor ceramics having better characteristics by improving the spinel based-NTC thermistor ceramics [6,7,10]. However, theoretically the NTC thermistor ceramic can still be explored from the known ceramics such as CuFe<sub>2</sub>O<sub>4</sub> spinel.

The CuFe<sub>2</sub>O<sub>4</sub> ceramics have been being developed as magnetic materials [11-13] and catalyst [14-16]. However, the CuFe<sub>2</sub>O<sub>4</sub> ceramics potentially, have capability of being NTC thermistors due to their semiconductive property. By evaluating the CuO-Fe<sub>2</sub>O<sub>3</sub> phase diagram [17], it can be predicted that a ceramic from mixture of CuO and Fe<sub>2</sub>O<sub>3</sub> (written as CuO-Fe<sub>2</sub>O<sub>3</sub>) sintered at 1100 °C may have different microstructures depending on their composition. Each microstructure will have its own electrical characteristic. It is interesting to know the relation between this microstructure and its electrical characteristic in order to find an alternative thermistor ceramic. So far, a study on formation of the thermistor ceramic from the mixture of CuO and Fe<sub>2</sub>O<sub>3</sub> with different compositions at 1100 °C has not been reported yet. Hence, that is the reason of why the study was carried out here. In this study the ceramics were designed to have three different microstructures namely two phase microstructure containing CuFe<sub>2</sub>O<sub>4</sub> and liquid phases, one phase microstructure containing CuFe<sub>2</sub>O<sub>4</sub> solid solution, and two phase microstructure containing CuFe<sub>2</sub>O<sub>4</sub> solid solution and hematite phase. The electrical characteristic of these ceramics in relation to their microstructures and crystal structure was the main topic of this study.

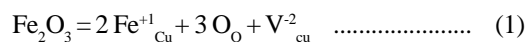
## EXPERIMENTAL METHOD

Powder of CuO and powder of Fe<sub>2</sub>O<sub>3</sub> with composition of (50 mole % CuO and 50 mole % Fe<sub>2</sub>O<sub>3</sub> as composition 1), (40 mole % CuO and 60 mole % Fe<sub>2</sub>O<sub>3</sub> as composition 2) and (34 mole % CuO and 66 mole % Fe<sub>2</sub>O<sub>3</sub> as composition 3) were mixed homogeneously in ethanol medium. The powder mixtures were dried at 80 °C for 24 hours, afterward. The three kinds of mixtures were then calcined at 800 °C for 2 hours. After being calcined, the powders were crushed and sieved with a sieve of < 38 μm. The sieved powder was then pressed with pressure of 3,9 ton/cm<sup>2</sup> into green pellets. The green pellets were sintered at 1100 °C for 2 hours in air with heating and cooling rates of 10 °C/minutes.

The crystal structure of the sintered pellets was analyzed with x-ray diffraction (XRD) using Kα radiation from Cu target. The microstructure of the pellets was investigated by an optical microscope. Before analyses by using an optical microscope, the pellets were ground, polished, and etched. The opposite-side surfaces of the sintered pellets were coated with Ag paste. After the paste was dried at room temperature, the Ag coated-pellets were heated at 500 °C for 10 minutes. The resistivity was measured at various temperatures from 25 °C to 100 °C in steps of 5 °C using two probes method and a computer controlled equipment.

## RESULTS AND DISCUSSION

Figure 1, Figure 2, and Figure 3 show the XRD profiles of CuFe<sub>2</sub>O<sub>4</sub> base-ceramic of composition 1, 2 and 3, respectively. The XRD profiles show that the structure of the ceramics of composition 1 and 3 is tetragonal after being compared to the XRD standard profile of CuFe<sub>2</sub>O<sub>4</sub> from JCPDS No. 22-1012 and the ceramic of composition 2 is cubic after being compared to the XRD standard profile of CuFe<sub>2</sub>O<sub>4</sub> from JCPDS No. 25-0283. No peak from second phase observed in the sample of composition 1 and 2. Regarding the sample of composition 1, the second phase may be in small concentration and smaller than the precision limit of the X-ray diffractometer used or the peak can not be differentiated from background or the cooling rate is slow enough so that the ceramic completely forms CuFe<sub>2</sub>O<sub>4</sub> at room temperature. According to the CuO-Fe<sub>2</sub>O<sub>3</sub> phase diagram, the ceramic with composition of 50 mole% CuO and 50 mole% Fe<sub>2</sub>O<sub>3</sub> may form CuFe<sub>2</sub>O<sub>4</sub> as the main phase and CuO as the second phase. The microstructure data may be used to evaluate whether the second phase is present or not in sample of composition 1. While regarding the sample of composition 2, it is possible that the mixture of CuO and Fe<sub>2</sub>O<sub>3</sub> has formed a solid solution of Cu<sub>1-x</sub>Fe<sub>2+x</sub>O<sub>4</sub> where x is the excess of Fe<sub>2</sub>O<sub>3</sub> dissolved. Additional peaks are seen in the XRD pattern of sample of composition 3. They are from the second phase of hematite (JCPDS No.33-0664). The reaction of the formation of the Cu<sub>1-x</sub>Fe<sub>2+x</sub>O<sub>4</sub> solid solution by equation 1 is as follow



where, Fe<sub>Cu</sub><sup>+1</sup> is the Fe<sup>+3</sup> ion occupies the Cu sub lattice, O<sub>O</sub> is the oxygen ion occupies the oxygen sub lattice and V<sub>Cu</sub><sup>-2</sup> is the Cu vacancy with 2- charge.

The formation of tetragonal spinel in the ceramics of composition 1 and composition 3 and the formation of cubic spinel in the ceramics of composition 2 indicate that the cooling rate is slow enough for the ceramics of composition 1 and 3, and fast enough for the ceramics of composition 2. According to G.F. Goya and H.R. Rechenberg [18], CuFe<sub>2</sub>O<sub>4</sub> ceramic will crystallize to cubic when the ceramic is cooled rapidly (high cooling

rate) and to tetragonal when it is cooled slowly (low cooling rate) from a relatively high temperature. The different crystal structure of the ceramics produced here may be due to different composition which has different thermodynamical property. The ceramics having second phases of composition 1 and 3 have crystal structure of tetragonal spinel and that is free from second phase of composition 2 has crystal structure of cubic spinel.

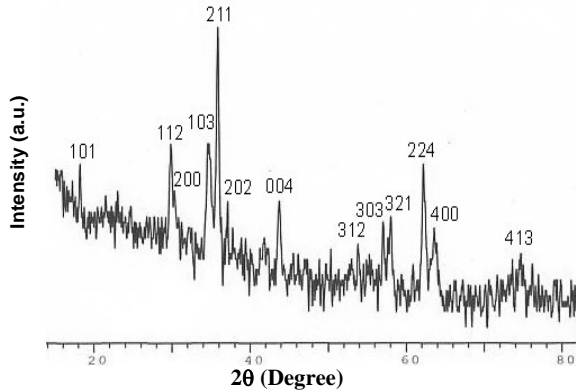


Figure 1. XRD profile of  $\text{CuFe}_2\text{O}_4$  base-ceramic of composition 1, showing a tetragonal spinel structure.

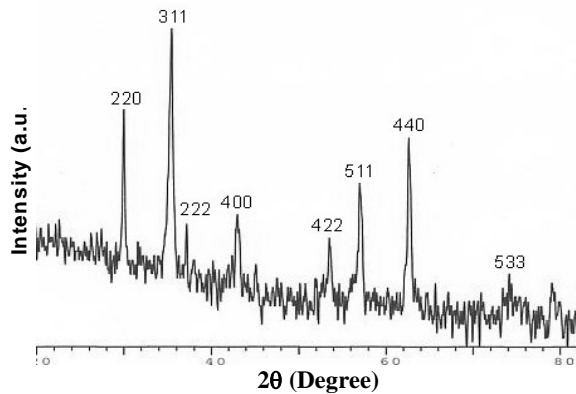


Figure 2. XRD profile of  $\text{CuFe}_2\text{O}_4$  base-ceramic of composition 2, showing a cubic spinel structure.

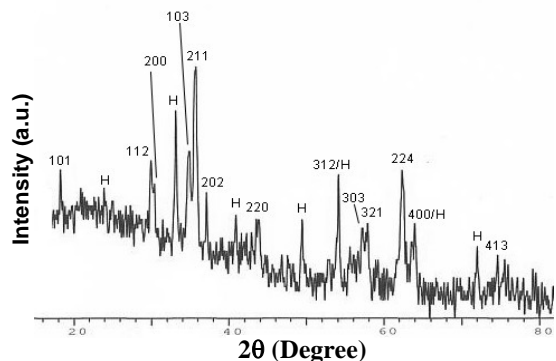
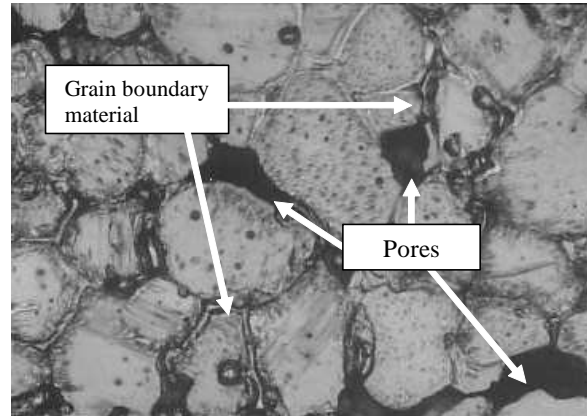


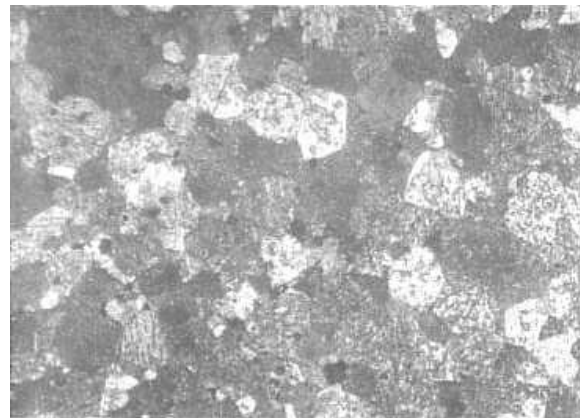
Figure 3. XRD profile of  $\text{CuFe}_2\text{O}_4$  base-ceramic of composition 3, showing a tetragonal spinel structure with additional peaks from hematite (H).

From Figure 4 and Figure 5 the effect of  $\text{SiO}_2$  addition on the microstructure cannot be known due to the small effect. However, it is clearly shown from Figure 6 that the addition of  $\text{SiO}_2$  decreases the size of

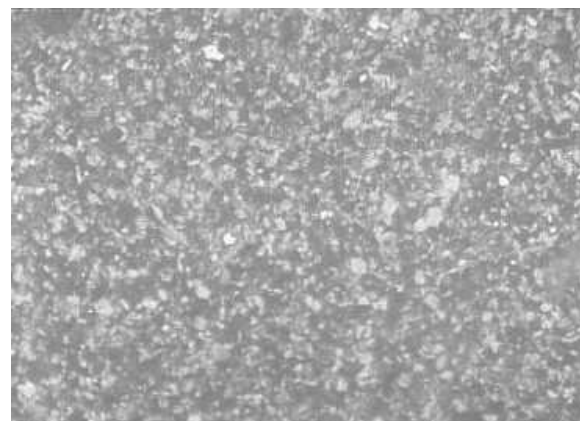
grains. The decrease of the grain size is due to the segregation of the  $\text{SiO}_2$  at grain boundaries. The electrical data of the  $\text{SiO}_2$  added- $\text{CuFe}_2\text{O}_4$  ceramics is shown in Figure 7 and Table 1.



a. Composition 1 (50 mole%  $\text{CuO}$ -50 mole%  $\text{Fe}_2\text{O}_3$ )



b. Composition 2 (40 mole%  $\text{CuO}$ -60 mole%  $\text{Fe}_2\text{O}_3$ )



c. Composition 3 (36m/o  $\text{CuO}$ -64m/o $\text{Fe}_2\text{O}_3$ )

Figure 4. Microstructure of  $\text{CuFe}_2\text{O}_4$  base-ceramic of composition 1, composition 2 and composition 3.

Figure 4 shows the microstructure of the ceramics of composition 1, composition 2 and composition 3, respectively. Figure 4a shows that the ceramic of composition 1 composing of (50 mole %  $\text{CuO}$  and 50 mole %  $\text{Fe}_2\text{O}_3$ ) forms a microstructure having rounded grains. This indicates that a liquid phase was

present during sintering in this ceramic. The presence of glassy grain boundary material in Figure 4a is the prove of the presence of the liquid phase. During cooling this liquid (all or a part) crystallized to CuFe<sub>2</sub>O<sub>4</sub> spinel which cannot be seen in the XRD profile of the ceramic of composition 1. Figure 4b. is the microstructure of the ceramic composition 2 (40 mole% CuO and 60 mole% Fe<sub>2</sub>O<sub>3</sub>). This ceramic has no second phase and contains polygonal grains. This feature shows that the ceramic of composition 2 is free from liquid phase during sintering. Different color (bright and dark) shown in Figure 4b., indicates different orientation of the grains. The Fe<sub>2</sub>O<sub>3</sub> excess forms a solid solution with CuO where Fe<sup>3+</sup> ions replace Cu<sup>2+</sup> ions to form Cu<sub>1-x</sub>Fe<sub>2+x</sub>O<sub>4</sub> ceramic. As shown in Figure 4c., the grains of the ceramic of composition 3 are very small. This is due to the presence of the Fe<sub>2</sub>O<sub>3</sub> excess as confirmed by XRD data which tends to segregate at the grain boundaries and inhibits grain growth during sintering. The segregated Fe<sub>2</sub>O<sub>3</sub> limits the movement of grain boundaries.

The electrical data of Figure 5 shows that the electrical characteristic of the ceramics of different compositions follows the NTC tendency expressed by equation 2. As can be seen from Figure 5, the experimental data fit the fitting curve. As shown in Table 1, the Fe<sub>2</sub>O<sub>3</sub> excess increases the room temperature resistivity (ρ<sub>RT</sub>) and thermistor constant (B). Compared to the ( B ) value for market requirement where B ≥ 2000 K, the value of B for our ceramics are relatively large. The room resistivity of our ceramics also fits that of market requirement where the value of the ρ<sub>RT</sub> of the market requirement is 10 Ohm.cm-10<sup>6</sup> Ohm.cm [3].

$$\rho = \rho_0 \exp.(B/T) \dots\dots\dots (2)$$

where, ρ = Electrical resistivity, ρ<sub>0</sub> = Electrical resistivity at infinite temperature, B is the thermistor constant and T is the temperature in Kelvin.

The small value of room temperature resistivity (ρ<sub>RT</sub>) of the ceramic of composition 1 is mainly caused by large grains belongs to the ceramic that formed due to the presence of liquid phase during sintering. The ceramic with large grains has higher mobility of charge carrier due to a small grain boundary area.

While the large room temperature resistivity of the ceramic of composition 3 is caused by the small grains created by the presence of the Fe<sub>2</sub>O<sub>3</sub> excess. The Fe<sub>2</sub>O<sub>3</sub> excess was segregated at grain boundaries and inhibited grain growth during sintering. The ceramic with small grains has many grain boundaries which act as scattering center for charge carrier. This microstructure yields short mean free path for the charge carrier, causing the resistivity becomes large.

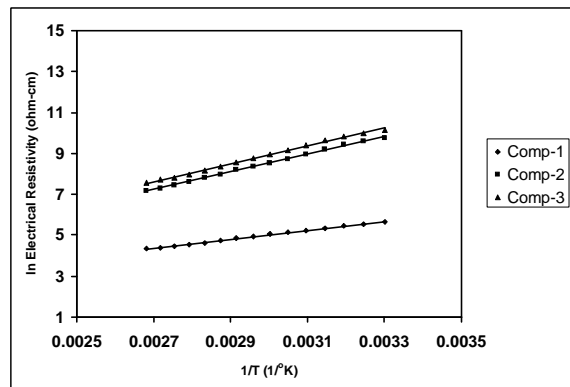


Figure 5. Electrical characteristic of CuFe<sub>2</sub>O<sub>4</sub> base-ceramic of composition 1, composition 2 and composition 3.

Table 1. Electrical characteristic of the CuFe<sub>2</sub>O<sub>4</sub> base-ceramics.

No.	Composition	B (°K)	α (%/°K)	ρ <sub>RT</sub> (Ohm-cm)
1.	1	2191	2.4	312
2.	2	4322	4.8	21272
3.	3	4397	4.9	32734

## CONCLUSION

The (CuO-Fe<sub>2</sub>O<sub>3</sub>) ceramics having three different microstructures have been successfully produced at sintering temperature of 1100 °C. Each microstructure has own electrical characteristic. The ceramics having second phase tend to crystallize in tetragonal spinel while that forming a solid solution of Cu<sub>1-x</sub>Fe<sub>2+x</sub>O<sub>4</sub> tends to crystallize in cubic spinel. The room temperature resistivity (ρ<sub>RT</sub>) and thermistor constant (B) tend to increase with the increase of Fe<sub>2</sub>O<sub>3</sub> concentration. The value of (ρ<sub>RT</sub>) of (312-32734 ohm.cm) and (B) of (2191-4397°K) of the (CuO-Fe<sub>2</sub>O<sub>3</sub>) ceramics made in this work fits the market requirement.

## ACKNOWLEDGMENT

The authors wish to acknowledge their deep gratitude to Saeful H. and M. Yamin for their help during experiment.

## REFERENCES

- [1]. BETATHERM Sensors [on line]. Available: <http://www.betatherm.com>
- [2]. EUN SANG NA, UNGYU PAIK and SUNG CHURL CHOI, *J. Ceram. Proc. Res.*, **2** (2001) 31
- [3]. YOSHIHIRO MATSUO, TAKUOKI HATA and TAKAYUKI KURODA, *US Patent* 4,324,702
- [4]. HYUNG J. JUNG, SANG O. YOON, KI Y. HONG and JEON K. LEE, *US Patent* 5,246,628
- [5]. KAZUYUKI HAMADA and HIROSHI ODA, *US Patent* 6,270,693

- [6]. K. PARK, *Mater. Sci. Eng.*, **B104** (2003) 9
- [7]. K. PARK and D.Y. BANG, *J. Mater. Sci.: Mater. in Elec.*, **14** (2003) 81
- [8]. SHOPIE GULEMET FRITSCH, JAOUAD SALMI, JOSEPH SARRIAS, ABEL ROUSSET, SHOPIE SCHUURMAN and ANDRE LANNOO, *Mater. Res. Bull.*, **39** (2004) 1957
- [9]. R. SCHMIDT, A. BASU and A.W. BRINKMAN, *J. Europ. Ceram. Soc.*, **24** (2004) 1233
- [10]. K. PARK and I.H. HAN, *Mater. Sci. Eng.*, **B119** (2005) 55
- [11]. J.Z. JIANG, G.F. GOYA and H.R. RECHENBERG, *J. Phys.: Condens. Mater*, **11** (1999) 4063-4078
- [12]. G.F. GOYA, H.R. RECHENBERG and J.Z. JIANG, *J. Mag. Magnet. Mater.* **218** (2000) 221
- [13]. C.R. ALVES, R. AQUINO, M.H. SOUSA, H.R. RECHENBERG, G.F. GOYA, F.A. TOURINHO and J. DEPEYROT, *J. Metas. Nanocrys. Mater.* **20-21** (2004) 694
- [14]. KAMEOKA SATOSHI, TANABE TOYOKAZU and TSAIAN, *Catal. Lett.*, **100** (2005) 89
- [15]. W.F. SHANGGUAN, Y. TERNAOKA and S. KAGAWA, *Appl. Catal. Part B*, **16** (1998) 149.
- [16]. R.C. WU, H.H. QU and H. HE. Y.B. YU, *Appl. Catal. Part B*, **48** (2004) 49
- [17]. ANONYMOUS, *Phase Diagram for Ceramist*, ASTM
- [18]. G.F. GOYA and H.R. RECHENBERG, *J. App. Phys.* **84** (1998) 1101